

The host galaxy of GRB 010222: The strongest damped Lyman- α system known.[★]

I. Salamanca^{1†}, L. Kaper¹, P. M. Vreeswijk¹, S. L. Ellison², E. Rol¹
 N. Tanvir³, R.A.M.J. Wijers⁴, P.F.L. Maxted⁵ and E. van den Heuvel¹,

¹*Astronomical Institute “Anton Pannekoek”, University of Amsterdam, Kruislaan 403, 1098 SJ Amsterdam, The Netherlands*

²*European Southern Observatory, Alonso de Cordova 3107, Vitacura, Casilla 19001, Santiago 19, Chile*

³*Department of Physical Sciences, University of Hertfordshire, College Lane, Hatfield AL10 9AB, United Kingdom*

⁴*Department of Physics & Astronomy, SUNY, Stony Brook, New York 11794-3800, U.S.*

⁵*Astrophysics Group, School of Chemistry & Physics, Keele University, Staffordshire ST5 5BG, United Kingdom*

Accepted ... Received ...; in original form: 2001 December 3

ABSTRACT

Analysis of the absorption lines in the afterglow spectrum of the gamma-ray burst GRB 010222 indicates that its host galaxy (at a redshift of $z=1.476$) is the strongest damped Lyman- α (DLA) system known, having a very low metallicity and modest dust content. This conclusion is based on the detection of the red wing of Lyman- α plus a comparison of the equivalent widths of ultraviolet Mg I, Mg II, and Fe II lines with those in other DLAs. The column density of H I, deduced from a fit to the wing of Lyman- α , is $(5 \pm 2) \times 10^{22} \text{ cm}^{-2}$. The ratio of the column densities of Zn and Cr lines suggests that the dust content in our line of sight through the galaxy is low. This could be due to either dust destruction by the ultraviolet emission of the afterglow or to an initial dust composition different to that of the diffuse interstellar material, or a combination of both.

Key words: Gamma-ray: burst - Galaxies: absorption lines

1 INTRODUCTION

Gamma Ray Bursts (GRBs), the most powerful cosmic explosions, are very important as probes of the high-redshift universe. This is due to several factors: (i) GRBs occur at cosmological distances, the most distant so far being at $z=4.5$ (GRB 000131, Andersen et al. 2000), (ii) they can be extremely bright and therefore could be seen (though for a very short period of time) up to redshift 20 (e.g. Wijers et al. 1998; Lamb & Reichart 2000), (iii) the burst and its afterglow illuminate the material situated between the GRB and the observer, providing an opportunity to study galaxies that otherwise would be too faint to be observed spectroscopically. This is particularly relevant for the host galaxies of GRBs where, in analogy to quasar (QSO) absorption line studies, the strengths of the absorption lines can be used to measure important properties, such as their gas content, dynamical structure, and metallicity. In addition, since they are transient phenomena, they do not cause

the large scale “proximity effect” of quasars, i.e. they do not modify their environment at large distances, although they are expected to do so in their immediate vicinity (see section 5), (iv) the currently most popular physical explanation of this phenomenon is the so-called fireball model (cf. Rees & Meszaros 1992) which is a relativistic explosion caused by either the collapse of a massive star (Woosley 1993; Paczynski 1998) or the merging of two compact objects (Lattimer & Schramm 1974). In the first case the rate of GRBs in the universe should be directly linked to the instantaneous star formation rate (SFR). This indeed seems to be supported by the observations, since the host galaxies of GRBs[†] are undergoing strong star-formation activity (e.g. Fruchter et al. 2001; Vreeswijk et al. 2001). Therefore, GRBs offer the potential to measure the cosmic star-formation rate (SFR) as a function of redshift.

In this paper we report on spectroscopic observations of the GRB 010222 afterglow taken ~ 23 hours after the burst. We present evidence that its host galaxy is a damped

[★] Based on observations made with the 4.2-m William Herschel Telescope, operated on the island of La Palma by the Isaac Newton Group in the Spanish Observatorio del Roque de los Muchachos of the Instituto de Astrofísica de Canarias.

[†] e-mail: isabel@science.uva.nl

[‡] Actually, this is true for bursts whose duration is longer than 2 seconds, since they are the only ones which have been localized up to now.

Lyman- α absorption (DLA) system with the strongest column density of neutral hydrogen and the lowest metallicity currently known. This has strong implications for both theories of the nature of GRBs and their host galaxies, and for the studies of DLA absorption systems. In particular, it shows that DLA systems with $N(\text{HI}) > 10^{22} \text{ cm}^{-2}$ do exist, and that the way to detect them may be by looking at GRB afterglow spectra rather than QSO absorption line spectra. This is of extreme importance because DLAs are key components of the universe at high redshift due to the fact that, although relatively rare, they account for most of the neutral gas available for star formation.

In section 2 we present the observations and describe the calibration procedures. In section 3 the reduced spectra are analysed, resulting in a detailed identification of the absorption lines, and the determination of the metallicity and dust content of the gas producing them. Finally, in section 4 we determine the nature of the galaxy hosting GRB 010222 and compare it to the host galaxies of other GRBs, as well as with other Mg II and damped Ly α absorption systems. The discussion and conclusions are presented in section 5 and section 6, respectively.

1.1 GRB 010222

GRB 010222 was discovered on February 22, 2001, at 7:23:30 U.T. by the Wide Field Camera (WFC) on board *BeppoSAX* (Piro 2001). This burst is one of the brightest bursts ever recorded, with a fluence of $(9.3 \pm 0.3) \times 10^{-5}$ in the energy range from 40 to 700 keV. Soon after its detection, an optical transient was discovered with coordinates RA = $14^{\text{h}}52^{\text{m}}12^{\text{s}}.55$ and DEC = $+43^{\circ}01'06''.2$ (J2000), and magnitudes $V \sim 18$ and $R = 18.4 \pm 0.1$ (Henden 2001; McDowell et al. 2001; Henden & Vrba 2001). A series of optical spectra of the afterglow taken shortly after the alert allowed the determination of the redshift of the host galaxy (Garnavich et al. 2001; Jha et al. 2001; Bloom et al. 2001; Castro et al., 2001), which is $z = 1.476$. For a cosmology with $H_0 = 65 \text{ km s}^{-1} \text{ Mpc}^{-1}$, $\Omega_m = 0.3$, $\Lambda = 0.7$, the luminosity distance is $D_L = 3.6 \times 10^{28} \text{ cm}$, and the isotropic energy output is $7.8 \times 10^{53} \text{ erg}$ (in 't Zand et al. 2001), which makes GRB 010222 the third most energetic of all GRBs with known redshift.

With regard to the host galaxy, observations of GRB 010222 at mm- and sub-mm-wavelengths have led to the interpretation that it is vigorously forming stars at a rate of $\sim 500 M_{\odot} \text{ yr}^{-1}$ (Frail et al. 2001), whilst in the optical and near-infrared it is a faint ($V = 26.0 \pm 0.1$) compact (FWHM $\sim 0''.15$) galaxy (Fruchter et al. 2001).

2 WHT SPECTRA OF THE OPTICAL AFTERGLOW

We obtained optical spectra of the afterglow of GRB 010222 on 2001 February 23, at 06:03:08.976 U.T. (i.e. 22.66 hours after the burst) with the double spectrograph ISIS at the 4.2-m *William Herschel Telescope* (WHT), of the Isaac Newton Group (ING) situated at ‘‘El Roque de los Muchachos’’ observatory, La Palma, Spain. We used an EEV12 and a TeK CCD (charged coupled device) as detectors, together with the B300B and R158R gratings in the blue and red arm,

respectively. The total exposure time was 50 minutes. The spectral resolution, as measured from the width of the arc lines, is 3.3 \AA in the blue arm, and 5.8 \AA in the red arm. The nominal wavelength coverage for the blue arm is from 2728 to 6267 \AA . However, the camera optics in the blue arm suffer from vignetting, resulting in a reduced effective wavelength range (3042 to 5954 \AA). The red arm covers the range from 6140 to 9115 \AA . The log of the observations is listed in Table 1.

The data were debiased, divided by a normalized flat field and extracted following standard procedures in IRAF[§]. The spectra were then calibrated in wavelength using Ar-Cu arc spectra. A comparison between the observed and theoretic wavelength of the Balmer series in the standard star gives an average error of 1.15 \AA in the blue spectrum, and 0.91 \AA in the red spectrum. Sky emission lines were removed by subtraction of the average sky background spectrum next to the object. However, in the region redwards of $\sim 7600 \text{ \AA}$ the sky subtraction is difficult and remnant sky emission lines are left. This does not affect the subsequent analysis as we have not used this part of the spectrum in our analysis. Finally, the flux calibration was performed using standard star BD+26 $^{\circ}$ 2606. The atmospheric extinction was applied using the mean extinction curve for La Palma. We present the final spectrum in Figs. 1 and 2.

3 ANALYSIS OF THE ABSORPTION LINES

3.1 Line identification

We identified several absorption lines in the spectrum of the GRB 010222 afterglow, belonging to (at least) three different absorption systems at redshifts $z=1.476$, $z=1.156$ and $z=0.927$ (Jha et al. 2001; Masetti et al. 2001; Castro et al. 2001). Actually, the GRB 010222 afterglow is one of the richest in terms of line detections; a compilation of absorption lines detected in GRB afterglow spectra can be found in Vreeswijk et al. (2001). In this paper we will concentrate on the system at the highest redshift, which we will adopt as belonging to the host galaxy of GRB 010222.

The host galaxy’s absorption lines and their identification are compiled in Table 2, together with the rest-frame equivalent width (EW) and some atomic parameters (the oscillator strength, f , and the ionization potential of the ion, IP, in eV). For comparison, we have listed the EW published by Jha et al. (2001) and Masetti et al. (2001). The lines that we could not identify (neither at redshift 1.476, nor at the other two redshifts) are listed in Table 3.

It is important to determine whether the lines are saturated or not, which is difficult given the low resolution of our spectrum. Most of the absorption lines are expected to have a doppler broadening less than a few tens of km s^{-1} , which is much less than the spectral resolution ($\sim 220 \text{ km s}^{-1}$). Therefore, we have compared the observed ratio of the line intensities to the theoretical one, which is given by the ratio of their oscillator strengths. Furthermore, the absorption

[§] IRAF is distributed by the National Optical Astronomy Observatories, which are operated by the Association of Universities for Research in Astronomy, Inc., under cooperative agreement with the National Science Foundation.

Table 1. Log of the spectroscopic observations of the afterglow of GRB 010222. The data were taken on 2001 February 23, about 22.66 hours after the burst. The total exposure time is 50 minutes.

Instrument	CCD/Grism	Spect. range (\AA)	Spect. resol. ^a ($\text{\AA} / \text{km s}^{-1}$)
ISIS Blue arm	EEV12 / B300B	3042 - 5954	3.3 / 220 km s^{-1}
ISIS Red arm	TeK / R158R	6140 - 9115	5.8 / 230 km s^{-1}

^aAs measured from the FWHM of the arc lines

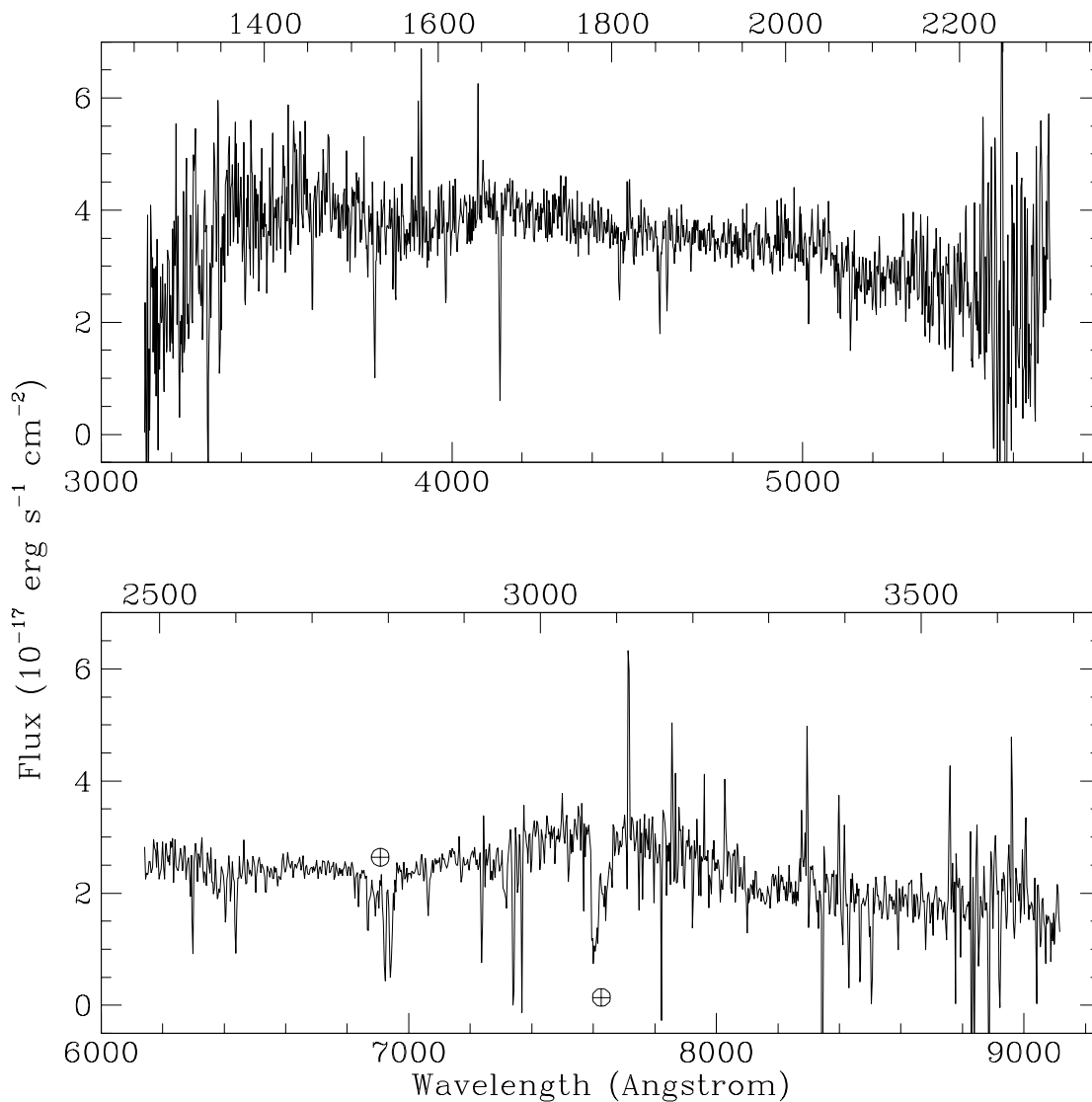


Figure 1. The optical spectrum of the afterglow of GRB 010222. For each panel, the observed wavelength is given at the bottom, and at the top, the wavelength at the host galaxy rest-frame (i.e. corrected by red-shift $z=1.476$). The spectrum includes many, mostly saturated, absorption lines which can be identified with common resonance lines at the redshift of the host galaxy ($z = 1.476$) and at two other absorption systems at redshifts ($z = 1.156$ and 0.927). The telluric absorption lines are marked with \oplus . At the redshift of the host galaxy, the center of the Lyman- α line should be located at $\sim 3011 \text{ \AA}$, which is just outside the wavelength range covered by our spectrum. However, we can see its red wing extending up to 3400 \AA (observed wavelength). We do not detect the interstellar graphite feature at 2175 \AA (rest-frame); the origin of the “bump” in the continuum around 7600 \AA is unclear.

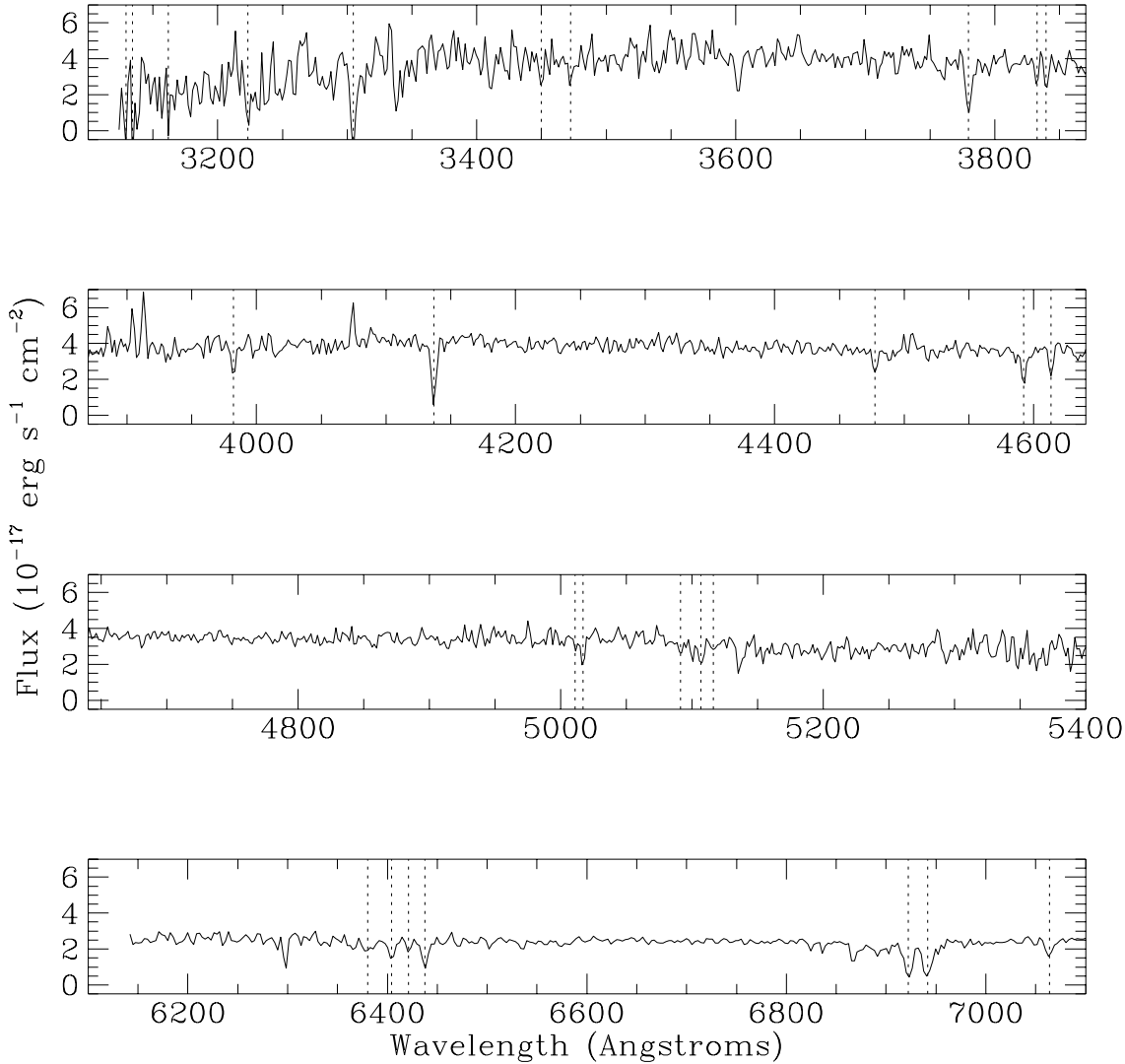


Figure 2. The optical spectrum of GRB 010222. We zoom in those areas which contain the lines listed in Table 2 and we marked them with a dotted line. The signal-to-noise per resolution element is ~ 13 .

lines with an equivalent width larger than $\sim 0.5 \text{ \AA}$ are most likely saturated (see for example Pettini et al. 2001). Accordingly, most of the absorption lines detected in the afterglow spectrum of GRB 010222 are actually saturated.

3.2 Detection of Lyman- α at $z=1.476$

The strongest line in the spectrum of GRB 010222's afterglow is actually Lyman- α , of which we can see its red wing extending up to $\sim 3400 \text{ \AA}$ (observer's frame) or $\sim 1370 \text{ \AA}$ (rest-frame). The center of Lyman- α should be at 3010.8 \AA in the observer's frame, which is just outside the wavelength region covered by our spectrum, close to the atmospheric and instrumental cut-off. We have checked that this feature is not due to instrumental effects, such as flat fielding or vignetting. For this purpose, we have compared the spec-

trum of GRB 010222 afterglow to that of the standard star, which was observed right after the exposure of GRB 010222 was finished. We can see in Fig. 3 that the feature that we identify as the red wing of Lyman- α is absent in the standard star spectrum and that the vignetting starts at wavelengths shorter than $\sim 3000 \text{ \AA}$ (observer's frame) or $\sim 1210 \text{ \AA}$ (rest-frame). This is what we expect according to the technical documentation published by the ING group (Garcia Lorenzo 2000). We have multiplied both spectra by an arbitrary constant, so they can be plotted in the same diagram, and binned them so that their general shape is more clear.

Consequently, we are confident that the feature observed at the blue end of the spectrum of GRB 010222's afterglow is the red wing of the damped Lyman- α absorption line of the host galaxy.

Table 2. Absorption lines identified at $z = 1.476$. The first column lists the observed wavelength, the second the identification, the third the redshift, and the fourth the equivalent width in the rest-frame of the host galaxy, i.e. divided by $(1+z)$. The error on the equivalent width is estimated by varying the location of the continuum. The error in the wavelength position is ~ 1.15 Å for the blue spectrum and 0.91 Å for the red spectrum. For comparison, we list in the fifth and sixth columns the equivalent width published by Jha et al. (2001) and by Masetti et al. (2001). The next columns are the oscillator strength of the transition, f (taken from Bergeson & Lawler 1993; Morton 1994, 2001; Savage & Sembach 1996; Bergeson et al. 1996; Vernor 1996 and Schectman et al. 1998), and the ionization potential of the corresponding ion, IP, in eV. Finally, in the last column, we mention whether the line is as well detected in absorption line systems towards quasars (e.g. Jannuzi et al. 1998), and two supernovae, SN 1987A (Blades et al. 1988) and SN 1993J (Marggraf & Boer 2000).

Obs. λ (Å)	Identification	Redshift	Eq. Width (Å)	EW Jha (+4.9 h)	EW Mas (+1day)	f	IP eV	detected as well
3129.2	Si II 1260.42	1.483	1.54 ± 1.18			1.007000	8.151	qso, 87A, 93J
3134.4	Si II* 1264.74	1.478	1.74 ± 0.20			0.903400	8.151	87A
3161.9	C I 1277.24	1.475	0.98 ± 0.07			0.096650	0	87A
3223.3	O I 1302.17	1.475	0.94 ± 0.03			0.048870	0	qso, 87A, 93J
3304.7	C II* 1334.53 ^a	1.476	2.34 ± 0.03			0.1278	11.26	qso, 87A
3449.8	Si IV 1393.76	1.475	0.67 ± 0.04			0.5280	33.49	qso, sn87A, 93J
3472.3	Si IV 1402.77	1.475	0.44 ± 0.01			0.2620	33.49	qso, 87A, 93J
3779.7	Si II 1526.71	1.476	1.65 ± 0.17	1.4 ± 0.4	1.2 ± 0.3	0.12700	8.151	qso, 87A, 93J
3832.4	C IV 1548.20	1.475	0.52 ± 0.10			0.190800	47.89	qso, 87A, 93J
3839.5	C IV 1550.78	1.476	0.71 ± 0.14	1.9 ± 0.4^f	2.3 ± 0.2	0.09522	47.89	qso, 87A, 93J
3982.3	Fe II 1608.45 ^b	1.476	0.67 ± 0.15			0.0580	7.87	qso, 87A
4136.9	Al II 1670.79	1.476	1.49 ± 0.09	1.1 ± 0.3	1.1 ± 0.3	1.800	5.986	qso, 87A
4477.4	Si II 1808.01 ^c	1.476	0.56 ± 0.02	0.5 ± 0.3	0.7 ± 0.3	0.00218	8.151	qso, 87A, 93J
4592.2	Al III 1854.72 ^d	1.476	0.73 ± 0.09			0.5390	18.83	qso, 87A, 93J
4613.3	Al III 1862.79	1.477	0.72 ± 0.07			0.2680	18.83	qso, 87A, 93J
5011.2	Zn II 2026.14	1.473	0.21 ± 0.24	1.0 ± 0.3	0.6 ± 0.2	0.489000	9.394	qso, 87A, 93J
5017.0	Mg I 2026.48	1.476	0.62 ± 0.02			0.1120	0	qso, 87A, 93J
5091.4	Cr II 2056.25	1.476	0.22 ± 0.07			0.1050	6.766	qso, 87A
5107.1	Zn II 2062.66	1.476	0.31 ± 0.03	0.7 ± 0.2	1.1 ± 0.2	0.256000	9.394	qso, 87A
	+Cr II 2062.23					0.0780	6.766	qso, 87A
5116.4	Cr II 2066.16 ^e	1.476	0.38 ± 0.33			0.05150	6.766	87A
6380.2	Mn II 2576.88	1.477	1.21 ± 0.40	0.7 ± 0.2	0.5 ± 0.2	0.3508	7.435	qso, 87A
6404.4	Fe II 2586.65	1.476	1.42 ± 0.68	1.5 ± 0.2	0.8 ± 0.3	0.069125	7.87	qso, 87A, 93J
6421.4	Mn II 2594.50	1.476	0.57 ± 0.38	0.7 ± 0.2	0.8 ± 0.3	0.2710	7.435	qso, 87A
6437.7	Fe II 2600.17	1.476	2.16 ± 0.70	1.9 ± 0.2	1.9 ± 0.2	0.2390	7.87	qso, 87A, 93J
6922.3	Mg II 2796.35	1.476	3.33 ± 1.27	3.0 ± 0.2	2.8 ± 0.2	0.6123	7.646	qso, 87A, 93J
6941.7	Mg II 2803.53	1.476	3.82 ± 1.65	2.7 ± 0.2	3.4 ± 0.3	0.3054	7.646	qso, 87A, 93J
7063.6	Mg I 2852.96	1.476	1.32 ± 0.89	0.9 ± 0.2	1.0 ± 0.3	1.81000	0	qso, 87A

^a The line of C II 1334.53 Å is broad (155 km s^{-1} after correction for the instrumental profile). It is also observed as a broad feature in the spectrum of SN 1987A (Blades, Wheatley, Panagia et al. 1998).

^b The line of Fe II 1608.45 Å is identified by Masetti et al. (2001) as Zn II 2062 Å at $z = 0.926$, but in this case we should observe Zn II 2026 Å as well, which we do not.

^c The Si II 1808.01 Å line should be accompanied by another one at 1816.93 Å, but the latter is contaminated by a sky emission line.

^d Note that this line is identified by Masetti et al. (2001) as being Fe II 2383 Å at $z = 0.926$.

^e This line is too strong which makes its identification uncertain. Maybe this line is blended with some other line.

^f The separate doublet components are not resolved, hence the equivalent width corresponds to the sum of both components.

3.3 Measuring the column densities

The average redshift, based on the metal lines, of the absorption-line system with the highest redshift is 1.467 (we have not taken into account the blends of Zn II + Cr II). According to Castro et al. (2001) there is some substructure in the gas forming these lines, with a separation of 106 km s^{-1} . The spectral resolution of our spectrum does not enable us to resolve this, and therefore we can only deduce the global properties of the galaxy or region where the GRB has taken place.

To measure the equivalent width, we used the routine `splot` within IRAF. The line was integrated with respect to the local continuum, by just summing the flux over a given

wavelength interval. No gaussian fitting was done, except in the few cases where the lines were partially blended, or the local continuum was noisy. In these cases, we checked the obtained EW by fitting a single Gaussian to the lines, yielding consistent results. To estimate the error on the EW measurement, we varied the position of the local continuum. The final value of the EW is the average of all measurements, while the error is conservatively taken as the difference between the highest and the lowest values obtained. The results are given in Table 2, where we have listed the EW published by Jha et al. (2001) and Masetti et al. (2001) too. In most cases, the three independently obtained values are consistent within the errors. However, in two cases the values do not agree: (a) the C IV doublet at 1548, 1550 Å which

Table 3. Unidentified lines. The equivalent width is as measured in the observer's frame.

Observed λ (Å)	Equivalent Width (Å)
3138.3	2.69 \pm 0.18
3178.5	2.32 \pm 0.07
3410.9	2.27 \pm 0.31
3709.8	0.78 \pm 0.03
4389.6	0.57 \pm 0.17
4488.6	0.53 \pm 0.07
4518.1	0.58 \pm 0.03
4525.2	0.32 \pm 0.00
4633.9	1.49 \pm 0.26
4681.2	0.63 \pm 0.01
4856.7	0.91 \pm 0.46 ^a
4859.6	(sum)
4914.0	0.45 \pm 0.03
5100.3	0.55 \pm 0.02
7340.1	7.02 \pm 0.11
7519.9	1.59 \pm 0.27
8504.5	7.63 \pm 0.37

^a This line is blended with the line at 4859.6 Å.

can be due to the fact that we resolve it, while Jha et al. (2001) and Masetti et al. (2001) do not; (b) the Zn II + Cr II 2026 Å blend, but again this can be explained by a difference in the spectral resolution: if we add the equivalent width of Mg I 2026 Å line to that of the Zn/Cr blend, then the values agree well.

3.3.1 HI column density

We have deduced the column density of H I by fitting a Voigt profile to the red wing of Lyman- α . For that purpose, we corrected the spectrum for redshift, and normalized the continuum to unity. Subsequently, we produced model profiles of damped absorption lines, for three values of $N(\text{H I})$: 3×10^{22} , 5×10^{22} and 7×10^{22} cm^{-2} , and compared them with the observed Lyman- α wing. Even though the observed spectrum is noisy and only part of the line profile is covered, a large value of $N(\text{H I})$ is required to match the observed red damping wing. The value we have adopted is $N(\text{H I}) = (5 \pm 2) \times 10^{22}$ cm^{-2} . This is formally (i.e. within the errors) consistent with the value deduced from X-ray observations, $(2.5 \pm 0.5) \times 10^{22}$ cm^{-2} (in 't Zand et al. 2001).

3.3.2 Column density of the other lines

As we have discussed earlier, most of the other lines seem to be saturated, and are, therefore, not suited to calculate their column density. We limit ourselves to those lines that are very likely *not* saturated. These are the Zn II and Cr II lines, given their intrinsic low cosmic abundance and the small value of the oscillator strength. Possibly the lines of Fe II 1608 Å, and Mn II 2594 Å are unsaturated too, but nevertheless, we regard the abundances determined from these transitions as lower limits.

In order to deduce the equivalent widths of the individual lines in the Zn + Cr blend, we start by measuring the EW of Zn II 2026 Å which is mainly dominated by Zn⁺, and the EW of Cr II 2056 Å which is not blended. The total EW of Zn II + Cr II 2026 Å is 0.21, but the contribution of Cr II 2026 Å can be neglected, because the ratio of the oscillator strengths of Cr II 2056 Å to Cr II 2026 Å is ~ 22 . Therefore, we assume that the EW of Zn II 2026 Å is 0.21 Å. This implies that the EW of Zn II 2062 Å is ~ 0.11 Å. Since the total EW of the Zn II + Cr II 2062 Å blend is 0.31 Å, then the EW of the Cr II 2062 Å becomes ~ 0.2 Å. The EW of the Cr II 2066 Å line has a very large error (87% relative error). Therefore, this line has not been taken into account to deduce the column density of Cr⁺.

Once we know the EW, we calculate N_{col} using the following relationship, valid in the limit of weak lines, between the (rest-frame) equivalent width and the column density (Scheffler & Elsasser 1987):

$$N_{\text{col}} = 1.131 \times 10^{12} \times \frac{\text{EW}}{\lambda^2 f} \text{ cm},$$

where f is the oscillator strength of the transition, and λ the wavelength in cm.

In the subsequent analysis, we have taken for each ion (Zn II, Cr II, Fe II, and Mn II) the average N_{col} of the individual transitions, if more than one unsaturated line could be measured. We assume that the abundance of each element X is closely approximated by X⁺ because the second ionisation potential is above 13.6 eV. The results are summarized in Table 4 and discussed in the following sections.

4 THE HOST GALAXY OF GRB 010222:

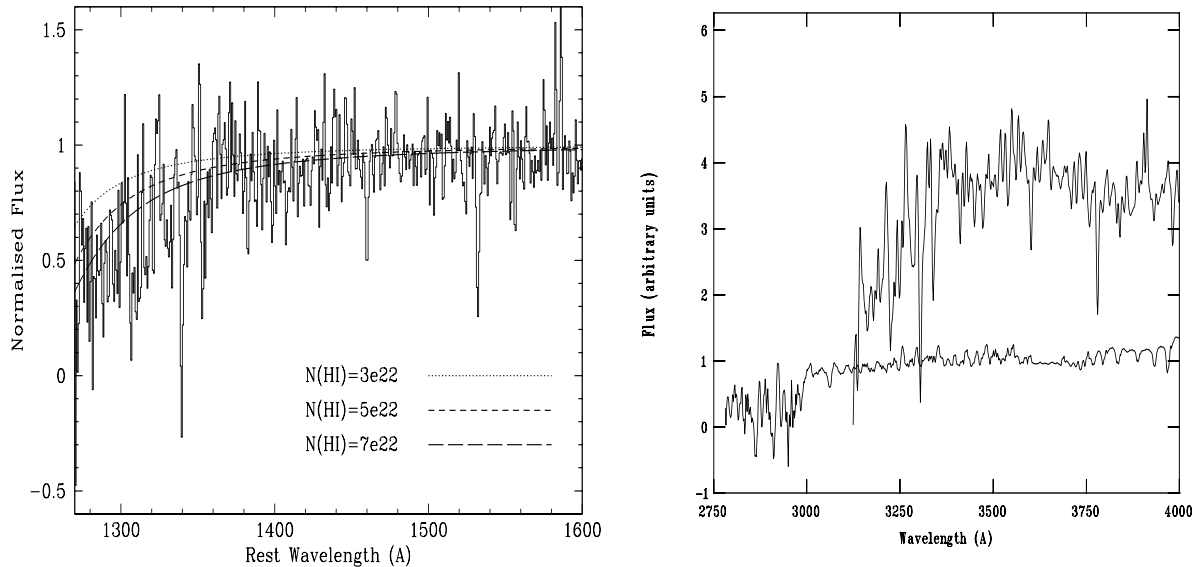


Figure 3. Evidence that the host galaxy of GRB 010222 is a damped Lyman- α system. **Left:** Our blue spectrum clearly shows the red wing of Lyman- α , which is matched with three Voigt profiles corresponding to a column density of neutral hydrogen of 3×10^{22} , 5×10^{22} and $7 \times 10^{22} \text{ cm}^{-2}$. Before the fitting, the spectrum has been corrected for redshift and the adjacent continuum normalized to unity. **Right:** The spectrum of GRB 010222 (top) is shown next to that of the standard star (bottom); the feature that we identify as the red wing of Lyman- α is not present in the spectrum of the standard star. Both spectra have been multiplied by an arbitrary constant so that they can be displayed in the same panel, and they have been binned so that their general trend is more obvious.

A DAMPED LYMAN- α SYSTEM

An absorption system is classified as a damped Lyman- α (DLA) system if the column density of neutral hydrogen is larger than $2 \times 10^{20} \text{ cm}^{-2}$. The column density of H I in the host galaxy of GRB 010222 is $N(\text{H I}) = (5 \pm 2) \times 10^{22} \text{ cm}^{-2}$. This, *by definition* makes the host galaxy of GRB 010222 a damped Lyman- α system. Further support to the classification of the host galaxy as a DLA comes from the analysis of Mg I, Mg II, and Fe II lines. According to Rao & Turnshek (2000), if the absorption system has $\text{EW}(\text{Mg II } 2796) > 0.6 \text{ \AA}$ and $\text{EW}(\text{Fe II } 2600) > 0.5$, it has 50% probability of being a DLA system. This is obviously the case for GRB 010222, as already pointed out by Masetti et al. (2001). Furthermore, all DLA systems in the Rao & Turnshek sample have Mg II 2796, 2803 \AA doublet ratios below 1.5, as is the case for GRB 010222 (Fig. 5). The relationship between $\text{EW}(\text{Mg II } 2796)$ versus $\text{EW}(\text{Fe II } 2600)$ also indicates that the host galaxy of GRB 010222 is a DLA: On the one hand both measured EWs are larger than 0.6 \AA , and on the other hand their ratio is ~ 1.5 , very close to the average value of 1.45 deduced by Rao & Turnshek (2000) (Fig. 5).

Furthermore, the equivalent widths of other low ionization lines in the spectrum of GRB 010222 are quite large compared to those of absorption-line systems present in QSO spectra. For example, the EW of Si II 1526 \AA is $1.65 \pm 0.17 \text{ \AA}$, while the values measured in the sample of Steidel & Sargent (1992) range from 0.02 to 1.87 \AA . Equally strong are the lines of Zn II 2026, 2062 \AA and Cr II 2026, 2056, 2062 \AA . If we compare for example their EW with those of the data collected by Pettini and collaborators (1994, 1997 and 1999), we see, again, that GRB 010222 has the highest values (even though it has the lowest metallicity, see later).

In order to estimate the metallicity and dust-to-gas ratio we compare the abundances of elements that are known

to be little depleted onto dust to that of refractory elements that are easily depleted on to dust grains. The best elements for such purpose are Zn (not depleted) and Cr, Mn, Fe and Ni (large depletion). Therefore, Zn is a good indicator of the metallicity, whilst Cr, Mn, Fe and Ni can be used to measure the dust content (for a more extended analysis of why these elements are useful to study the metallicity and dust content, see for example Pettini et al. 1990).

We adopt the usual notation, i.e.

$$[X/H] = \log \frac{N_{\text{col}}(X)}{N_{\text{col}}(H)}_{\text{GRB}} - \log \frac{N_{\text{col}}(X)}{N_{\text{col}}(H)}_{\odot} = \log \delta(X), \quad (1)$$

where $\delta(X)$ is the depletion of element X, or in other words, the fraction of element X in gas form, relative to its solar meteoritic abundance. The latter values have been taken from Savage & Sanders (1996).

For the zinc abundance, and thus a measure of the enrichment of the gas by metals, in the host of GRB 010222 we find a value of $[\text{Zn}/\text{H}] = -2.3 \pm 0.5$, indicating that the host galaxy has a very low metallicity, about 200 times less than the solar fractional Zn abundance. If we adopt $N(\text{H I}) = 2.5 \times 10^{22} \text{ cm}^{-2}$ (in 't Zand et al. 2001) then $[\text{Zn}/\text{H}]$ becomes -2.01 , about a factor 100 below solar, thus the host galaxy would still be amongst the most metal poor DLAs known. The lowest metallicity claimed up to now in DLAs is $[\text{Zn}/\text{H}] = -2.07 \pm 0.1$ (Molaro et al. 2001).

The dust content of the host galaxy can be deduced by comparing the Zn abundance to the abundance of some refractory elements:

$$[X/\text{Zn}] = \log \left(\frac{\delta(X)}{\delta(\text{Zn})} \right) \approx \log \left(\frac{f_{\text{gas}}}{f_{\text{gas}} + f_{\text{dust}}} \right) \quad (2)$$

where X is Cr, Fe or Mn, $\delta(X)$ its gas-phase abundance, and f_{gas} and f_{dust} are the fraction of element X in gas and dust

respectively. The value of $[X/Zn] = -0.3$ corresponds to the case where the fraction of X in dust is equal to the fraction of X contained in gas form ($f_{\text{gas}} = f_{\text{dust}}$). The results are summarized in Table 4. The abundances of Zn, Cr and Mn are consistent with each other, while that of Fe is slightly smaller.

A few words of caution before reaching any conclusion: The iron line FeII 1608 Å has an EW slightly larger than 0.5 Å, and therefore could be saturated, so its abundance should be regarded as a lower limit. The same applies to Mn, which in addition has a nucleosynthetic pattern that is not well understood, so we may be seeing effects of nucleosynthesis, and not of depletion on dust (Pettini et al. 2000). Also, it is important to realize that there might be effects due to the ionization of the gas caused by the local UV radiation field of OB stars and/or of the GRB itself. These effects would raise the value of $[Zn/Cr]$ which could mimic the absence of dust (Howk & Sembach 1999). However, further observational proof of the lack of dust in the host of GRB 010222 is the absence of the “2175 Å dip”, which is usually attributed to graphite dust grains and detectable down to $A_V \sim 0.1$ mag (see also Jha et al. 2001 and Masetti et al. 2001).

In order to compare the host of GRB 010222 with DLAs detected in QSO spectra, we have compiled the data published by Pettini and collaborators (1994, 1997 and 1999). In Fig. 4 we plot the column density of neutral hydrogen, $N(\text{HI})$, versus the Zn abundance $[Zn/H]$ (i.e. the metallicity) and the abundance of Cr^+ (indicator of the dust content) versus that of Zn^+ . Clearly, the host of GRB 010222 is exceptional in a number of ways. First, the low value of the metallicity is what one would expect from the extrapolation of the apparent correlation between $N(\text{HI})$ and the metallicity. There is some controversy regarding the reality of such correlation. Dust bias in DLA selection is one of the possible explanations for the absence of high column density, metal rich absorbers. A more plausible explanation is a cross-sectional bias against intercepting the center of galaxies. For a more detailed discussion we refer the reader to Ellison et al. 2001 (and references therein). Second, the abundances of Zn and Cr are the lowest in the whole sample. The correlation of Zn and Cr abundances is caused by the fact that they are both Fe-peak elements and are produced by similar nucleosynthetic reaction pathways. In Galactic stars, Zn and Cr actually track each other very closely, hence any departure from $[Cr/Zn]=0$ indicates depletion onto dust. If there was no depletion on to dust we would expect a one-to-one ratio in Fig 4. Instead, we observe a scatter of points below this line which is due to the presence of dust.

4.1 Other cases of DLAs in host galaxies of GRBs

This is not the first time that a GRB host galaxy has been confirmed as a damped Lyman- α system. Jensen et al. (2001) detected Lyman- α in the afterglow spectrum of GRB 000301C, and deduced a neutral hydrogen column density $\log N(\text{HI}) = 21.2 \pm 0.5 \text{ cm}^{-2}$, qualifying the host galaxy of GRB 000301C as a DLA. Another case where the line of Lyman- α is as well detected is the host galaxy of GRB 000926, where the column density of neutral hydrogen is $\log N(\text{HI}) \sim 21.3 \text{ cm}^{-2}$ (Fynbo et al. 2001). Although

both cases have $N(\text{HI})$ lower than in GRB 010222, they are still at the high end of the range found for typical DLAs.

It is useful to compare these results with those of Galama & Wijers (2001). From the analysis of the X-ray spectra of GRBs afterglows, they find evidence for high column densities ($\gtrsim 3 \times 10^{21} \text{ cm}^{-2}$) of circumburst material. The X-ray analysis has the advantage that it measures the column density of all atoms, irrespective of whether they are in gas or dust. However, at 1-2 keV rest-frame energies, the X-rays only measure the abundance of elements whose K edge is at or below that energy (roughly elements with $Z < 10$) and therefore one needs to know the metallicity in order to deduce $N(\text{HI})$. The usual practice is to assume solar metallicity which means that the real $N(\text{HI})$ could be even larger, supporting the idea that GRBs always happen in DLA systems.¶

Furthermore, analysis of the equivalent widths of MgII 2796, 2803 Å, MgI 2853 Å and FeII 2600 Å lines provides further support to the idea that the sites of GRB explosions are DLA systems. We have taken from the literature the EWs of those lines seen in GRB afterglow spectra and added these points to the diagrams (figs. 24 and 25) presented in Rao & Turnshek (2000). The results are shown in Fig. 5. It is evident that not only the host of GRB 010222 would qualify as a DLA on the basis of these diagrams, but also the hosts of GRB 970508, GRB 990123, GRB 000926, and possibly of GRB 990510 and GRB 991216 (Metzger et al. 1997; Andersen et al. 1999; Kulkarni et al. 1999; Castro et al. 2001; Vreeswijk et al. 2001). These results reinforce the idea that all GRB host galaxies are DLAs. In addition, Rao & Turnshek (2000) conclude, apart from the fact that all the systems in their sample with $\text{EW}(\text{MgI } 2582) > 0.7 \text{ Å}$ are DLAs, that there is no particular correlation between the EWs of MgII 2796 Å and MgI 2582 Å lines. However, this changes if we add the values for the GRB mentioned before: there is a clear trend for both EW being proportional to each other (see Fig. 6).

5 DISCUSSION

From the analysis of the optical spectrum of the afterglow of GRB 010222, we conclude that its host galaxy is a DLA absorption line system, with the strongest column density of neutral hydrogen and the lowest metallicity ever known, and with low dust content. On the other hand, based on the bright millimetre and sub-millimetre constant emission ($3.74 \pm 0.53 \text{ mJy}$ at 350 GHz), Frail et al. (2001) conclude that the host galaxy of GRB 010222 is a dusty galaxy with an intense burst of star formation ($\sim 500 \text{ M}_{\odot} \text{ yr}^{-1}$) while in the optical and near-infrared it is a blue sub-luminous galaxy.

There is an apparent contradiction, because Pettini et al. (1999), based on the lack of metallicity evolution from $z=0.5$ to $z=3.5$, concluded that DLAs do not trace the bulk

¶ In principle, when calculating $N(\text{HI})$, one should account for any intervening galaxies. Typically, those values will be similar to our own galaxy at high latitude, a few times 10^{20} cm^{-2} , which means that if one finds such high values, $N(\text{HI}) > 10^{22} \text{ cm}^{-2}$, it is most likely due to the host galaxy.

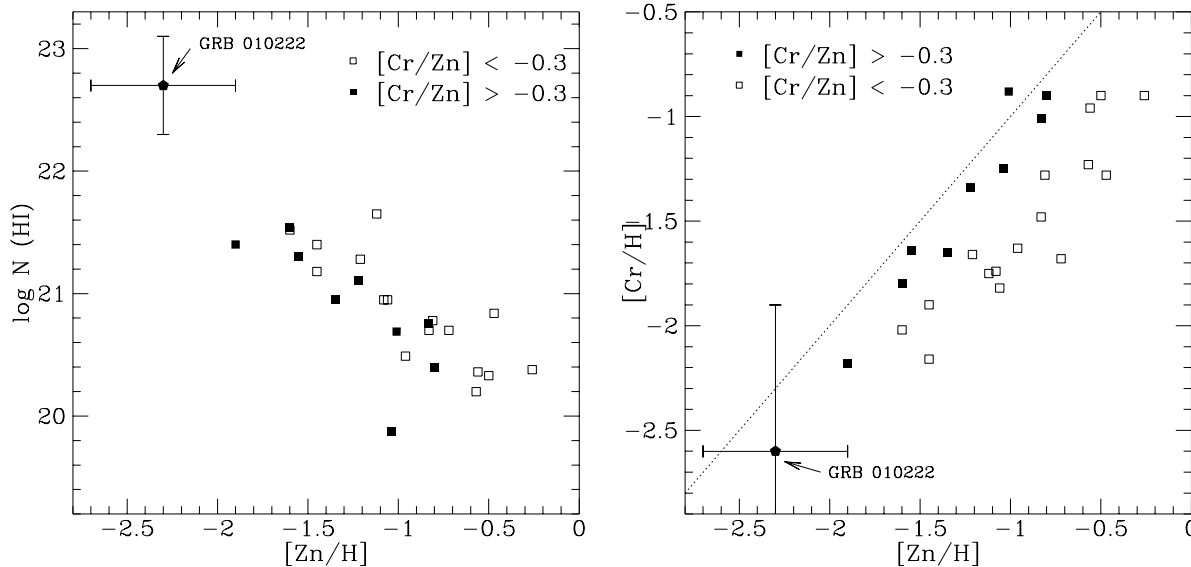


Figure 4. The host galaxy of GRB 010222 has the highest column density of HI and the lowest metallicity of the whole sample of DLAs. The data of the latter have been taken from Pettini et al. (1994, 1997 and 1999). The values of the abundances of Zn and Cr and of the column density of HI are what one would expect from an extrapolation of the correlations seen in both diagrams. A word of caution however: the correlation between $N(\text{HI})$ and $[\text{Zn}/\text{H}]$ is thought to be due to selection effects; there is no physical reason why there should not be absorption systems with a large $N(\text{HI})$ and high metallicity (see more details in text). The dotted line in the right diagram corresponds to the one-to-one correlation between the abundances of Zn and Cr that we would observe in the total absence of dust. Filled squares correspond to DLA systems with low dust content and open squares to systems with high dust content. The filled pentagon represents the host of GRB 010222. The errors in the Pettini sample vary from 1 to 20 per cent for $N(\text{HI})$, and from 0.2 to 0.4 dex for the abundances of Zn and Cr.

Table 4. Abundances and dust content in the host galaxy of GRB 010222. The column densities of Zn and Cr are obtained by averaging the results for the individual transitions Zn II 2026,2062 ÅÅ and Cr II 2056,2062 ÅÅ respectively. The column density of Mn and Fe has been obtained from a single transition, Mn II 2594 Å and Fe II 1608 Å. We assume that the abundance of each element can be approximated by the abundance of its first ionised ion, since the second ionisation potential is in all cases greater than 13.6 eV. For comparison, we list as well the range of abundances of these elements through different lines of sight in our Galaxy (see Savage & Sembach 1996 and references therein). Solar meteoritic abundances are taken from Savage & Sembach (1996).

Ion	N_{col} cm^{-2}	$[\text{X}/\text{H}]$ 010222	$[\text{X}/\text{Zn}]$ 010222	$\frac{f_{\text{dust}}}{f_{\text{gas}}}$	$[\text{X}/\text{H}]$ Halo	$[\text{X}/\text{H}]$ Disk+Halo	$[\text{X}/\text{H}]$ Warm Disk	$[\text{X}/\text{H}]$ Cool Disk
Zn ⁺	$(1.25 \pm 1.64) \times 10^{13}$	-2.3 ± 0.4	-	-	~ 0	~ 0	~ 0	~ 0
Cr ⁺	$(6.21 \pm 2.46) \times 10^{13}$	-2.6 ± 0.7	-0.34	~ 1.2	$(-0.38, -0.63)$	$(-0.72, -0.88)$	$(-1.04, -1.15)$	$(-2.08, -2.28)$
Mn ⁺	$> (3.53 \pm 2.35) \times 10^{13}$	$> -2.7 \pm 0.9$	-0.43	~ 1.7	$(-0.47, -0.72)$	(-0.66)	$(-0.85, -0.99)$	$(-1.32, -1.45)$
Fe ⁺	$> (5.05 \pm 1.13) \times 10^{14}$	$> -3.5 \pm 0.6$	-1.26	~ 17	$(-0.58, -0.69)$	$(-0.80, -1.04)$	$(-1.19, -1.24)$	$(-2.09, -2.27)$

of star-forming galaxies at these redshifts. Indeed, low redshift imaging studies (e.g. Le Brun et al. 1997) have shown that DLAs represent a wide range of morphological types. At higher redshifts, the low spin temperatures inferred from the 21 cm absorption line studies indicate that DLAs rarely represent massive galaxies and may be more analogous to metal-poor dwarfs (Chengalur & Kanekar 2000). On the other hand, the properties (column density, profile shapes, velocity dispersion and number of components) of Mg II lines seen in the spectra of QSOs seen at $z \sim 1.5$ are very similar to those observed in η Carina nebula. This means that these lines could be associated with an expansion event, like superbubbles driven by star formation (Danks 1999). However, Bond et al. (2001), after comparing the kinematics and redshift evolution of strong Mg II absorbers, conclude that

superwinds and star-forming galaxies can account for a substantial fraction of these, but not for DLAs which show different kinematics and no red-shift evolution.

Furthermore, DLA systems having $N(\text{HI}) > 10^{22} \text{ cm}^{-2}$ are very rare. In fact, to our knowledge, the host of GRB 010222 is the only one known. One of the explanations often suggested was that such systems would have a large dust content and therefore would be missed in optical surveys, but this cannot be the dominant effect because the survey of radio selected QSOs (and therefore circumvent the dust issue) by Ellison et al. (2001) did not find any DLA with a large $N(\text{HI})$. Another possible reason proposed by Schaye (2001a) is that clouds having such high column densities have a large fraction of molecular hydrogen, and such clouds are much smaller and shorter lived

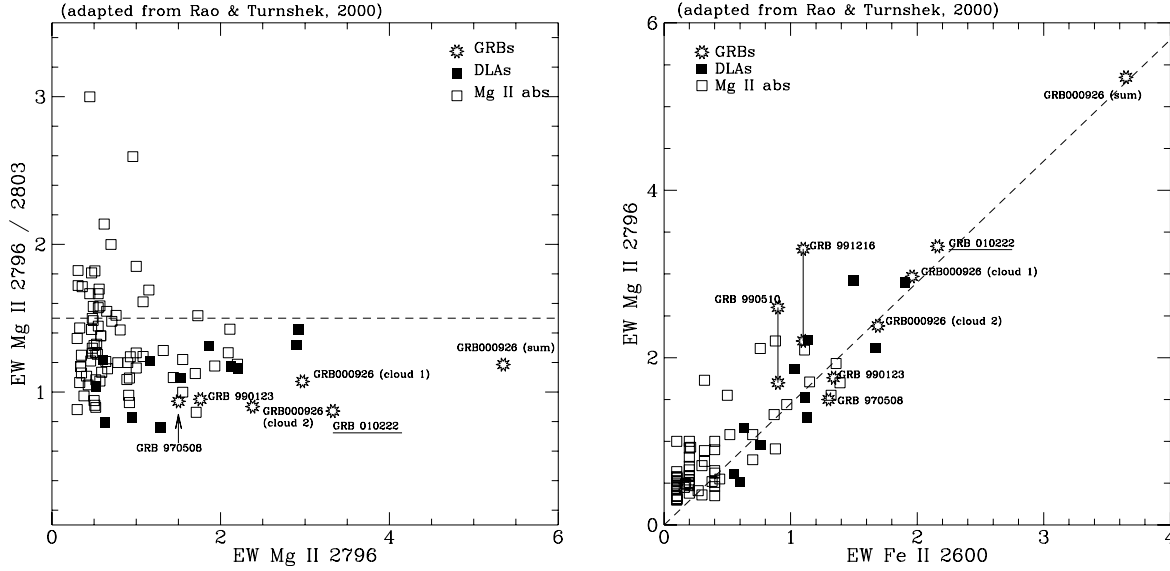


Figure 5. Are all GRB host galaxies damped Lyman- α systems? **Left:** The ratio of the equivalent width of the two Mg II doublet lines is below 1.5 for all the confirmed DLA systems in the sample of Rao & Turnshek (2000) and for those GRB for which this ratio has been measured (see label in figure). **Right:** Another indication that GRB host galaxies are DLAs: The equivalent width of Mg II 2796 Å is correlated to that of Fe II 2600 Å for the DLA systems of the sample of Rao & Turnshek (2000). The dotted line corresponds to the correlation given in Rao & Turnshek (2000). The GRB host galaxies for which this information is available follow this correlation. Moreover, all GRB hosts have equivalent widths of Fe II 2600 Å larger than 0.8 Å, and of Mg II 2796 Å larger than 2 Å. When the individual components of the Mg II lines were not resolved, two points are drawn in the diagram connected by a vertical line: the upper value is the total measured EW and the lower value is the EW divided by two.

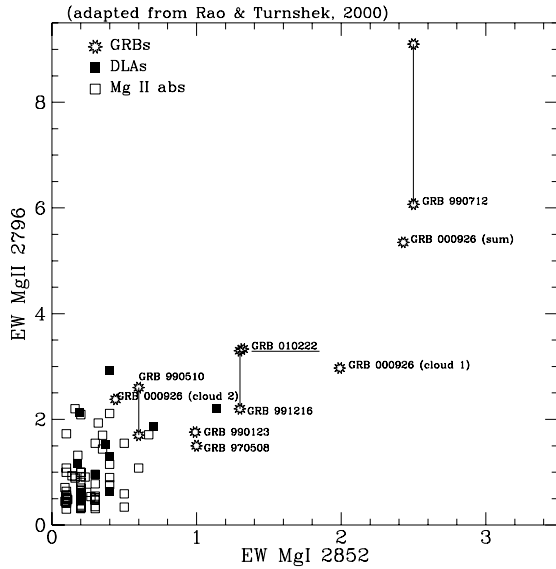


Figure 6. Relationship between the equivalent width of Mg II 2796 Å and that of Mg I 2852 Å. There is a clear trend for both quantities being correlated, that is not evident if one takes only into account the DLA systems of the Rao & Turnshek (2000) sample. The dots joined with a vertical line correspond to those cases where the Mg II doublet lines were blended: the upper value is the total measured EW and the lower value is the EW divided by two.

than clouds with low molecular fractions. Furthermore, at high redshift, there is a large population of compact galaxies with high star formation rates and large-scale outflows (called Lyman Break Galaxies, LBG), whose spectra resemble those of DLA systems seen through the line of sight to-

wards QSOs. These sight-lines will most likely intersect the outer parts of the galaxy, while the LBGs will probe the inner parts of the galaxy (for a detailed discussion see Schaye 2001b). The cross-section of such clouds will be very small, therefore making the chance bisection of a background QSO

unlikely. If GRB 010222, and GRBs in general, are associated with young, violent star formation regions, that is, with giant molecular clouds, which most likely have large $N(\text{HI})$, then the place to look for high column density DLAs is the spectra of the GRB afterglows, instead of those of QSOs.

Another issue of controversy is dust. To explain the fact that the optical/UV emission of the host galaxy is faint compared to the sub-millimetre emission, Frail et al. (2001) propose obscuration by dust. However, if the system had a high content of dust, there should be a higher amount of extinction and a larger depletion of certain elements, in particular Cr, than the one observed (see section 4). One possible explanation is that the dust is destroyed by the UV and X-ray radiation from the GRB and its afterglow. According to Fruchter et al. (2000), the X-ray emission of the burst can destroy dust (by grain charging mainly) within the first minutes out to 20 pc. Also, according to Waxman & Draine (2000), the UV flash of the burst can sublimate dust in the first hours after explosion. This would explain the low extinction and the absence of the 2175 Å feature which is due to small graphite particles (see also Galama & Wijers 2001 and references therein). However, according to Draine (2000) if the GRBs are associated with a molecular cloud, the UV flash would vibrationally excite H_2 which would then cause an absorption at wavelengths $\lesssim 1650$ Å which would be visible over tens of days. We do not observe such feature in our spectrum. Moreover, if dust is destroyed by the GRB and its afterglow emission, the ionization front should have affected the relative abundances of the different ions for the same element. Another factor that we must take into account is that the initial size distribution of dust particles could be different to that in the diffuse Galactic media, with a deficiency of small grains and an increase of large ones. This is what is expected in very dense environments -such as molecular clouds- where small particles are systematically removed (Kim 1994) and it is indeed observed in the Small Magellanic Cloud (Weingartner & Draine 2001, Welty 2001) and in some Seyfert galaxies (Maiolino et al. 2001). If this applies to the environment where the GRBs take place then the feature due to silicate grains at $9.7 \mu\text{m}$ should be absent as well.

A word of caution: the low value of $[\text{Zn}/\text{H}]$ that we find for GRB 010222 does not necessarily mean that its host galaxy is especially metal poor. It could just mean that cold, dense, giant molecular clouds are particularly depleted. Given the fact that the QSOs are unrelated to the absorption-line sites and the GRBs may not be, it is unclear whether the GRB host galaxies are special or only the GRB environments within hosts. The low resolution of our spectra does not allow us to disentangle these two cases. There is one case, GRB 000926, where Castro et al. (2001) find that the circumburst material is formed by two different clouds with a velocity separation of 168 km s^{-1} . In these two clouds the relative abundances of Zn and Cr are similar to each other, thus indicating that the metallicity and dust depletion are characteristic of the host galaxy as a whole, and ruling out the hypothesis of grain destruction in the vicinity of the burst. In the case of GRB 010222 there is also some sub-structure with a velocity separation of 106 km s^{-1} (Castro et al. 2001). If these subsystems had similar abundances, then the metallicity and dust content that we find would

be representative of the galaxy as a whole, and again, dust destruction by the burst itself would be ruled out.

6 CONCLUSIONS

The observational evidence points out that GRB 010222 has taken place in a damped Lyman- α system having the highest column density of neutral hydrogen and the lowest metallicity known up to now, and with low dust content. This result reinforces the idea that a small cross-section, and not dust, is the cause of not finding DLA systems having very large $N(\text{HI})$. If the system associated with GRB 010222 is not atypical, this means that we may be missing an important fraction of HI at cosmological distances which in turn may have an impact on Ω_{DLA} (i.e. the fraction of neutral gas in DLAs as a function of the closure density), although the exact contribution will depend on their cross section, which is unarguably small.

It is not clear whether the dust is destroyed by the GRB itself, or if its size distribution is different, being devoided of small particles. In the latter case the feature due to silicate grains at $9.7 \mu\text{m}$ should be absent also.

Finally, there is strong evidence that other GRB host galaxies (or at least their locations) are as well damped Lyman- α systems. Since they seem as well associated with star formation, we conclude that they may occur in a subclass of DLAs that *is* associated with active star formation.

ACKNOWLEDGEMENTS

I.S. and P.M.V. acknowledge support from NWO (post-doctoral grant no. 614.051.003 and Spinoza grant respectively). L.K. is supported by the Royal Academy of Arts and Sciences in The Netherlands (KNAW). We thank the staff at La Palma who performed the ToO observations.

REFERENCES

- Andersen M.I., et al. 1999, *Sci*, 283, 2075
- Andersen M.I. et al. 2000, *A&A*, 364, L54
- Bergeson S.D., Mullman K.L., Wickliffe W.E., Lawler J.E., Litzen U., Johansson S., 1996, *ApJ*, 464, 1044
- Bergeson S.D., Lawler J.E., 1993 *BAAS*, 183, 9204
- Bond N.A., Churchill C.W., Charlton J.C., Vogt S.S., 2001, *ApJ*, submitted (astro-ph/0108062)
- Blades J.C., Wheatley J.M., Panagia N. et al. 1988, *ApJ* 334, 308
- Bloom J.S., Djorgovski S.G., Halpern J.P., Kulkarni S.R., Galama T.J., Price P.A., Castro S.M., 2001, *GCN Circ.* 989
- Castro, S., et al. 2001, *GCN Circ.* 999
- Castro, S., Galama T.J., Harrison F.A., Holtzman J.A., Bloom J.S., Djorgovski, Kulkarni S.R., 2001, *ApJ*, submitted (astro-ph/0110566)
- Chengalur J.N., Kanekar N., 2000 *MNRAS*, 318, 303
- Danks A.C., 1999 *Ap&SS*, 269, 639
- Djorgovski S.G., Kulkarni S.R., Bloom J.S., Goodrich R., Frail D.A., Piro L., Palazzi E., 1998, *ApJ* 508, L17
- Draine B.T., 2000, *ApJ*, 532, 273
- Ellison S.L., Yan L., Hook I.M., Pettini M., Wall J.V., Shaver P., 2001, *A&A*, accepted (astro-ph/0109205)
- Frail D.A. et al. 2001, *ApJ*, accepted (astro-ph/0108436)
- Fruchter, A.S., Vreeswijk, P.M. et al. 2001, in prep.

- Fruchter A.S., Krolik J.H., Rhoads J.E., 2001, ApJ, accepted (astro-ph/0106343)
- Fynbo J. P.U., et al., 2001, proceedings of the conference “Light-houses of the Universe” held in Garching (Germany), August 2001 (astro-ph/0110603)
- Galama T.J., Wijers R.A.M.J. 2001, ApJ 549, 209
- Garnavich P.M., Pahre M.A., Jha S., Calkins M., Stanek K.Z., McDowell J., Kilgard R., 2001, CGN Circ. 965
- García-Lorenzo B., 2000, www.ing.iac.es/Astronomy/instruments/isis/isis_blue.html
- Henden A. 2001, GCN Circ. 961 & 962
- Henden A., Vrba F. 2001, GCN Circ. 967
- Howk J.C., Sembach K.R., 1999, ApJ, 523, 141
- in ’t Zand J.J.M., Kuiper L., Amati L. et al. 2001, ApJ, 559, 710
- Iverson R.J. et al. 2001, GCN Circ. 1004
- Jannuzi B.T., et al. 1988, ApJS 118, 1
- Jensen B.L., et al. 2001, A&A 370, 909
- Jha S. et al. 2001, ApJ, 554, L155
- Kim S., Martin P.G., Hendry P.D., 1994, ApJ, 422, 164
- Kulkarni S.R. et al., 1999, Nat, 398, 389
- Kulkarni, S., et al., 2001, GCN Circ. 996
- Lamb D.Q., Reichart D.E., 2000, ApJ, 536, 1
- Lattimer J.M., Schramm D.N. 1974 ApJ, 192, 145
- MacFadyen, A.I. & Woosley, S.E. 1999, ApJ, 524, 262
- Maiolino R., Marconi A., Salvati M., Risaliti G., Severgnini P., Oliva E., La Franca F., Vanzì L., 2001, A&A, 365, 28
- Marggraf O., de Boer K.S., 2000, A&A 363, 733
- Masetti N., et al. 2001, A&A 374, 382
- McDowell J., Kilgard R., Garnavich P.M. et al. 2001, GCN Circ. 963
- Metzger M.R., Djorgovski S.G., Kulkarni S.R., Steidel C.C., Adelberger K.L., Frail D.A., Costa E., Frontera F., 1997, Nat 387, 878
- Molaro P.M., Bonifacio P., Centurión M., D’Odorico S., Vladilo G., Santin P., Di Marcantonio, P., 2001, ApJ, submitted (astro-ph/0005098)
- Morton D.C., 1991 ApJS, 77, 119
- Morton D.C., 2001 ApJS, 132, 411
- Paczynski B., 1998 ApJ, 494, 45
- Pettini M., Boksenberg A., Hunstead R.W., 1990, ApJ 348, 48
- Pettini M., Smith L.J., Hunstead R.W., King D.L., 1994, ApJ, 426, 79
- Pettini M., Smith L.J., King D.L. Hunstead R.W., 1997, ApJ, 486, 665
- Pettini M., Ellison S.L., Steidel C.C., Bowen D.V., 1999, ApJ, 510, 576
- Pettini M., Ellison S.L., Steidel C.C., Shapley A.E., Bowen D.V., 2000, ApJ 532, 65
- Pettini M., Shapley A.E., Steidel C.C., Cuby J.-G., Dickinson M., Moorwood A.F.M., Adelberger K.L., Giavalisco M., 2001 ApJ, 554, 981
- Piro, L. 2001, GCN Circ. 959
- Rees M.J., Meszaros P., 1992, MNRAS, 258, L41
- Rao S.M., Turnshek D.A., 2000, ApJ Supl. Ser., 130, 1
- Savage B. D., Sembach K. R., 1996, ARA&A, 34, 279
- Schectman R.M., Povolny H.S., Curtis L.J., 1998, ApJ, 504, 921
- Scheffler H., Elsasser H. 1987, in “Physics of the Galaxy and Interstellar Matter”, ed. Springer-Verlag.
- Schaye J., 2001a, submitted (astro-ph/0109280)
- Schaye J., 2001b, ApJ 559, L1
- Steidel C.C., Sargent W.L.W., 1992, ApJ Supl. Ser. 80, 1
- Vernor 1996, Data Nuc Data tables 64,1
- Vreeswijk P.M., et al. 2001, ApJ 546, 672
- Vreeswijk P.M., et al., 2001, ApJ submitted
- Waxman E., Draine B.T., 2000, ApJ, 537, 796
- Weingartner J.C., Draine B.T., 2001, ApJ, 548, 296
- Welty D.E., Lauroesch J.T., Blades J.C., Hobbs L.M., York D.G., 2001, ApJ, 554, L75
- Wijers R.A.M.J., Bloom J.S., Bagla J.S., Natarajan, P., 1998, MNRAS, 294, 13
- Woosley S.E., 1993 ApJ, 405, 273

This paper has been produced using the Royal Astronomical Society/Blackwell Science L^AT_EX style file.